Improved Resistive Switching Performance through Donor-Acceptor Structure Construction in Memristors Based on Covalent Organic Framework Films

Dongchuang Wu, [a] Qiongshan Zhang, [c] Ning Gu, [b] Yang Cao, [c] Youyi Sun, [b]* Bin Zhang [c]* and Yu Chen[c]*

[a] School of Energy and Power Engineering, North University of China, Taiyuan 030051, China;

[b] School of Materials Science and Technology, North University of China, Taiyuan 030051, China;

[c] Key Laboratory for Advanced Materials and Joint International Research Laboratory of Precision Chemistry and Molecular Engineering, School of Chemistry and Molecular Engineering, East China University of Science and Technology, Shanghai 200237, China;

Materials

1,3,5-triformylphloroglucinol (TP) was synthesized following the previously reported literature protocols. [1] Tris(4-aminophenyl)amine (TAPA), acetic acid (CH_3COOH) and 1,3,5-triformylbenzene (TFB) were purchased from Macklin and used directly in the interfacial polymerization reaction. Dichloromethane (DCM), Ethanol, acetone, and 2-propanol were purchased from Aladdin. All compounds was used without further purification.

Instruments

Fourier transform infrared (FTIR) spectra were recorded by Spectrum 100 spectrophotometer (Perkin Elmer, Inc., USA). The scanning electron microscopy (SEM) images were recorded on a field emission scanning electron microscope (FESEM, Carl Zeiss Gemini) operating at an accelerating voltage of 3 kV. High magnification transmission electron microscopy (TEM) was performed using a JEOL-2100 (JEOL Ltd., Japan) TEM system operating at an accelerating voltage of 200 kV. ^{13}C crosspolarization/magic angle spinning solid-state nuclear magnetic resonance (CP/MAS ssNMR) experiments were performed on a Bruker AVANCE III 400 WB spectrometer operating at 100.62 MHz for ^{13}C using a double resonance 4 mm MAS NMR probe and a sample spinning rate of 10 kHz. The cross polarization time was 1 ms. The chemical shifts were referenced with adamantane. Atomic force microscopy (AFM) was measured on a Solver P47-PRO (NT-MDT Co., Moscow, Russia) microscope, and a Bruker Dimension Icon scanning probe microscope, respectively. Thermal gravimetric analyses (TGA) were performed on a Perkin-Elmer TGA-7 thermogravimetric analyzer in nitrogen atmosphere from ambient temperature to 800 ℃ at the rate of 10 ℃ min^{-1}. Powder X-ray diffraction patterns were recorded on

a Bruker D8 Advance diffractometer with Cu-Kα1 radiation (λ=1.5406 Å). UV–vis diffuse reflectance spectra (UV–vis DRS) were recorded at room temperature on a HITACHI U-4100 Spectrophotometer. 1H NMR spectra were recorded on a Bruker Avance 400 NMR spectrometer, operating at frequencies of 400 MHz using $CDCl_3$ as solvent. X-ray photoelectron spectroscopy (XPS) experiments were carried out on an AXIS Ultra DLD system from Kratos with mono Al Kα radiation (1486.6 eV) as X-ray source, the C 1s value was set at 284.6 eV for charge corrections.

Synthesis of triformylphloroglucinol (TP)[1]

To hexamethylenetetraamine (15 g, 108 mmol) and dried phloroglucinol (6 g, 49 mmol) under N_2 was added 90 mL trifluoroacetic acid. The solution was heated at 100 ºC for ca. 2.5 h. Approximately 150 mL of 3 M HCl was added and the solution was heated at 100 ºC for 1 h. After cooling to room temperature, the solution was filtered through Celite, extracted with ca. 350 mL dichloromethane, dried over magnesium sulfate, and filtered. Rotary evaporation of the solution afforded 1.48 g (7.0 mmol, 14%) of an off-white powder. ^{1}H NMR (300 MHz, CDCl3) δ 14.10 (s, 3H, OH), 10.14 (s, 3H, CHO) ppm;

Fabrication of the COF thin films

The COF films were fabricated via interfacial reaction between aldehyde and amine building blocks at room temperature and atmospheric pressure. TAPA (17.4 mg, 0.06 mmol) and TP (12.6 mg, 0.06 mmol) or TP (9.7 mg, 0.06 mmol) were dissolved in 100 ml of DCM as the organic phase. The TAPA and TP solutions were poured into a beaker together as the organic phase, and then pure water was slowly added onto the top surface of the DCM solution, leaving a stable DCM/water interface. Subsequently, 0.5 ml of aqueous acetic acid (3.0 M) was gently added into the aqueous phase as the catalyst. Afterward, the beaker was covered to keep it under a stable condition and avoid airflow. A transparent and smooth thin film was clearly observed at the interface between the two immiscible phases. After interfacial reaction for 3 days at room temperature, the water was pumped out slowly and the thin film was floated on the quiet DCM solution. The thin film was transferred to an ITO substrate, which had been carefully precleaned sequentially with deionized water, acetone, and 2-propanol in an ultrasonic bath for 15 min. And then it was rinsed several times by ethanol and DCM to wash away the residual monomers. In order to completely remove monomers, the film supported by ITO was immersed in DCM for 10h. The clean film was used to further characterizations and the fabrication of devices.

Device fabrication

The film supported by ITO was followed by the removal of the solvent under vacuum at 60°C overnight. Al top electrodes were deposited on the surface of active layer through a shadow mask at 10^{-7} Torr via E-beam evaporation. All electrical measurements were performed on a Keithley 4200 semiconductor parameter analyzer in ambient condition without any device encapsulation.

Energy levels calculation

The HOMO or LUMO levels and energy bandgaps of TAPA-TP can be electrochemically estimated from the equation. HOMO or LUMO = $-(E_{onset} - E_{ox(ferrocene)}) - 4.8$ using the onset potentials (vs. Ag/Ag^+) of the materials. Here, the reference energy level of ferrocene was considered as 4.8 eV. The onset oxidation potential of ferrocene was observed to be 0.38 V vs. Ag/Ag^+. The first oxidation and reduction potentials for TAPA-TP were found to be +0.98 V versus Ag/Ag^+ and -0.65 V versus Ag/Ag^+, respectively. As a result, the estimated HOMO energy level, and the LUMO energy level of TAPA-TP are -5.4V and -3.77V, respectively.

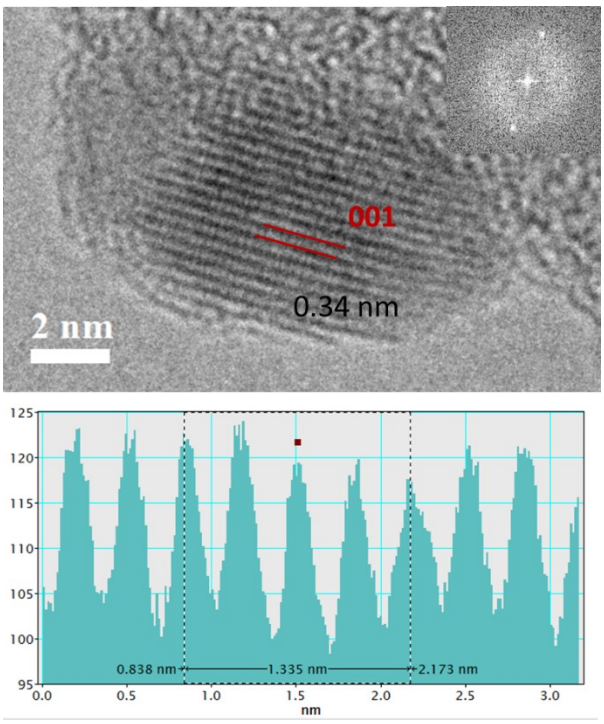

Figure S1. HRTEM image of (001) plane in TAPA-TP.

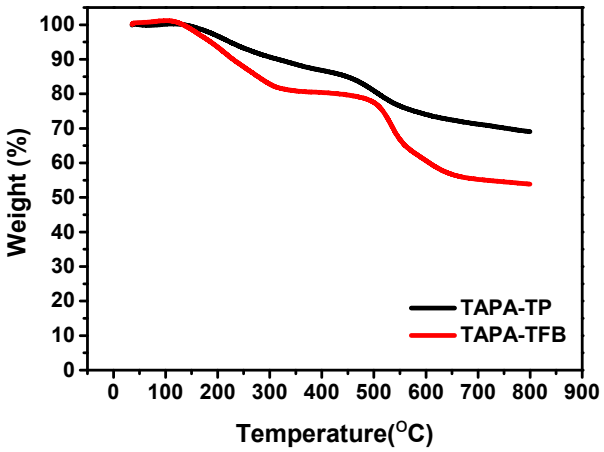

Figure S2. TGA curves of TAPA-TP and TAPA-TFB at a heating rate of 10 ºC min^{-1} under a nitrogen atmosphere.

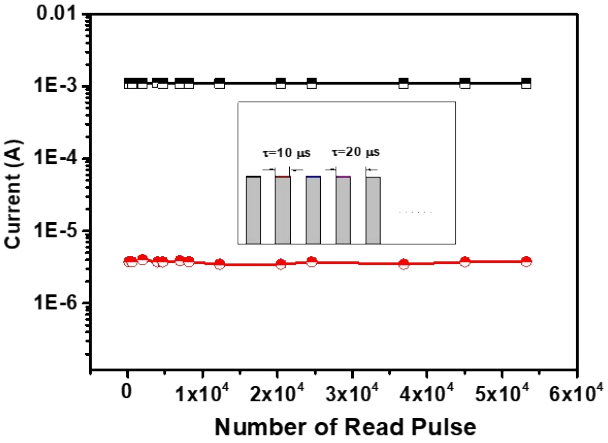

Figure S3. Effect of continuous read pulses of 0.1V (pulse width: 10 μs; pulse period: 20 μs)

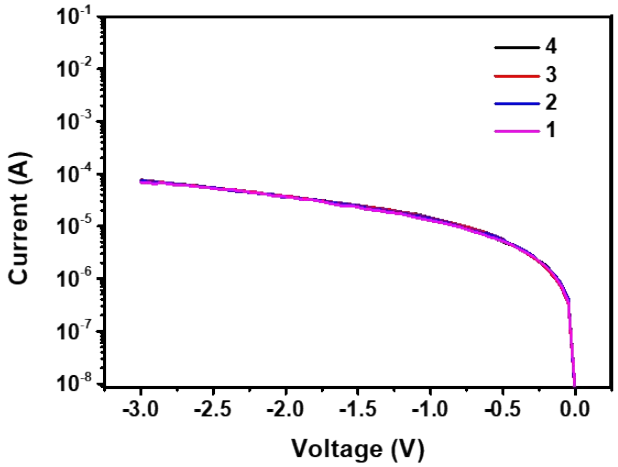

Figure S4. I–V characteristics of Al/TAPA-TP/ITO under negative voltage sweeps.

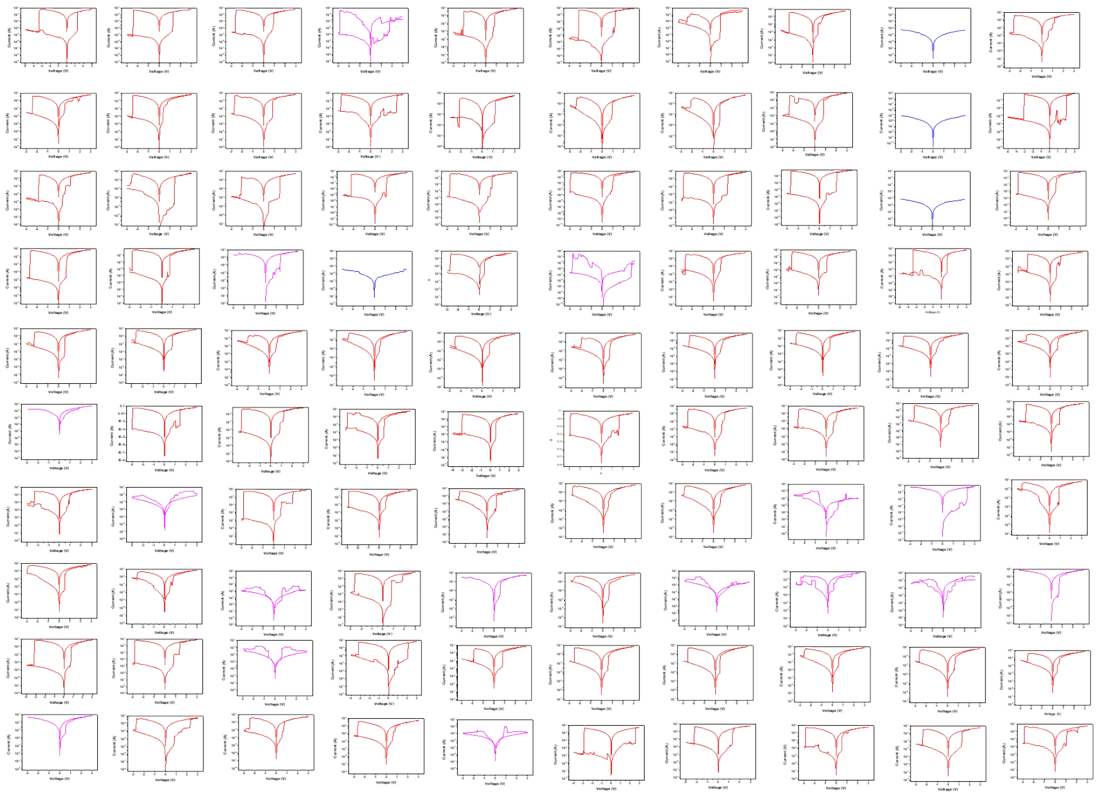

Figure S5. The I-V curves of 100 devices

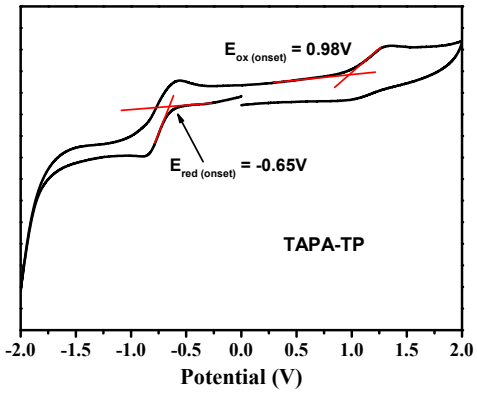

Figure S6. Cyclic voltammogram for TAPA-TP at ambient temperature. Scan rate: 100 mV s^{-1}. Reference electrode: Ag/AgCl. Electrolyte: Bu_4NPF_6 (0.1 M) in deaerated acetonitrile.

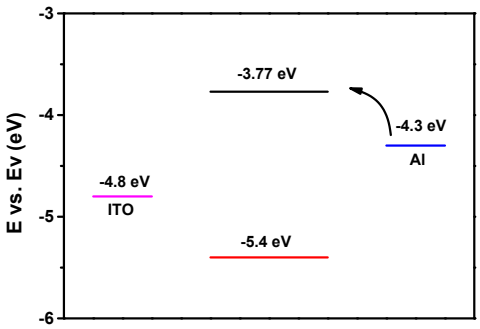

Figure S7. Energy levels of the TAPA-TP film and the electrodes

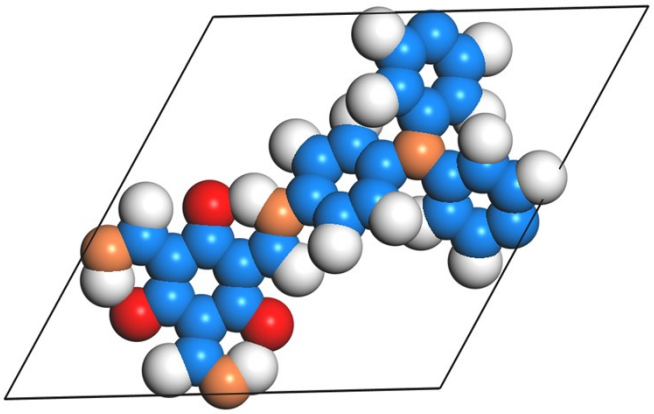

Figure S8. The eclipsed (AA) stacking mode of TAPA-TP

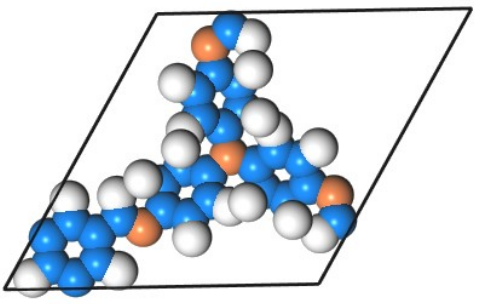

Figure S9. The eclipsed (AA) stacking mode of TAPA-TFB

Table S1. Fractional atomic coordinates for the eclipsed AA-stacking unit cell of TAPA-TP.

Space group	**P1**		
Calculated unite cell	a = b = 15.8604 Å, c = 3.4093 and α=β= 90^{o}, γ=60^{o}		
Atom	x	y	z
C1	0.272612	0.402344	0.299122
C2	0.212555	0.35713	0.298601
C3	0.25344	0.25289	0.257208
C4	0.358861	0.19227	0.261853
C5	0.422458	0.233322	0.263801
C6	0.377374	0.338254	0.302561
C7	0.43836	0.374866	0.37338
C8	0.396861	0.092757	0.310356
C9	0.114611	0.416736	0.373526
C10	0.460632	0.511154	0.501084
C11	0.428276	0.608198	0.384704
C12	0.489594	0.646153	0.413733
C13	0.583748	0.590917	0.576894
C14	0.610887	0.496929	0.727099
C15	0.552017	0.456724	0.683964
C16	0.614657	0.728228	0.556277
C17	0.521115	0.795293	0.69199
C18	0.480605	0.894748	0.628315
C19	0.534109	0.932055	0.436704
C20	0.63083	0.867208	0.335226
C21	0.669252	0.767501	0.386743
C22	0.751887	0.559514	0.574892
C23	0.817797	0.586819	0.71182
C24	0.917077	0.528616	0.66485
C25	0.955412	0.437674	0.488409
C26	0.891755	0.404765	0.387252
C27	0.792082	0.465391	0.422185
O1	0.233922	0.494774	0.309213
O2	0.19957	0.215112	0.229894
O3	0.51455	0.179579	0.243069
N1	0.404036	0.470172	0.417448
N2	0.492676	0.030316	0.337601
N3	0.053153	0.382359	0.397608
N4	0.650053	0.626177	0.587326
H1	0.327711	0.510956	0.371328
H2	0.532811	0.066375	0.290453
H3	0.088121	0.307694	0.32899
H4	0.356919	0.651732	0.245139

H5	0.463532	0.719977	0.302158
H6	0.680174	0.453864	0.877357
H7	0.576127	0.38323	0.801862
H8	0.478698	0.768932	0.848323
H9	0.407737	0.944102	0.738496
H10	0.674004	0.895173	0.191527
H11	0.743104	0.719684	0.289079
H12	0.790475	0.656025	0.854136
H13	0.965257	0.553214	0.774132
H14	0.920569	0.333548	0.254815
H15	0.745121	0.438909	0.322753
H16	0.516763	0.323982	0.39578
H17	0.087385	0.494239	0.418865
H18	0.34649	0.064827	0.335471

Table S2. Fractional atomic coordinates for the eclipsed AA-stacking unit cell of TAPA-TFB.

Space group	**P1**		
Calculated unite cell	a = b = 15.8479 Å, c = 3.4093 and α=β= 90^o, γ=60^o		
Atom	x	y	z
C1	0.738085	0.283336	0.395329
C2	0.675199	0.383001	0.380868
C3	0.581168	0.422821	0.224068
C4	0.554827	0.357248	0.071899
C5	0.615599	0.257703	0.100719
C6	0.707904	0.218548	0.272029
C7	0.37307	0.505832	0.381982
C8	0.273427	0.542466	0.395773
C9	0.208508	0.637399	0.271366
C10	0.247548	0.690665	0.099986
C11	0.347106	0.651986	0.071476
C12	0.412792	0.560078	0.22438
C13	0.495755	0.685167	0.379813
C14	0.532373	0.748138	0.392478
C15	0.62731	0.718042	0.267608
C16	0.680588	0.62568	0.096712
C17	0.641945	0.56481	0.069497
C18	0.550031	0.59113	0.222934
C19	0.756018	0.742821	0.382032

C20	0.802131	0.801855	0.406671
C21	0.746212	0.903999	0.409947
C22	0.791546	0.959832	0.409526
C23	0.893717	0.91352	0.41293
C24	0.949637	0.812311	0.409512
C25	0.903362	0.756491	0.410036
C26	0.054897	0.766094	0.386686
C27	0.7325	0.065072	0.386519
H1	0.810095	0.253743	0.523779
H2	0.699957	0.430618	0.492821
H3	0.484975	0.384999	0.931085
H4	0.592958	0.209179	0.975276
H5	0.420765	0.433502	0.494898
H6	0.243925	0.499997	0.524637
H7	0.198929	0.761841	0.974122
H8	0.374764	0.694146	0.930273
H9	0.423437	0.709865	0.493271
H10	0.489894	0.820147	0.521009
H11	0.751771	0.603029	0.970503
H12	0.684143	0.49491	0.928965
H13	0.948487	0.677171	0.40532
H14	0.666882	0.938239	0.405127
H15	0.927908	0.958616	0.410349
H16	0.804759	0.663314	0.417135
H17	0.085683	0.814733	0.42292
H18	0.652963	0.095923	0.4213
N1	0.514666	0.524682	0.216027
N2	0.664252	0.780369	0.316648
N3	0.109174	0.674365	0.320644
N4	0.770132	0.119223	0.321842

Table S3. The memory parameters of COF-based memristors.

Device structure	Memory effect	Turn-on voltage (V)	ON/OFF ratio	Switching mechanism	Reference
Ag /$2DP_{BTA+PDA}$/ ITO	Binary RRAM	0.9	＞10^5	Ag filament	R2
LiF/Al/PI-NT COF film/ITO	WORM	2.3	＞10^6	Electric-field-induced charge transfer	R3
Ag /COF-BT-TT/ ITO	Binary RRAM	1.3	10^5	Ag filament	R4
Ag /COF-5 film/ ITO	Binary RRAM	-0.94	10^3	Ag filament	R5
Au /$2DP_{TPAK+TAPB}$/ ITO	WORM	1.52	10^3	Electric-field-induced charge transfer	R6
Ag /SL-$2DP_{TAPB+TPOC8}$/ ITO	Binary RRAM	0.6	＜100	Ag filament	R7
Al/TFPB-PDAN/ITO	Binary RRAM	0.84	2.07×10^2	Electric-field-induced charge transfer	R8
Al/TAPA-TP/ITO	Binary RRAM	+0.9	7.39×10^2	Electric-field-induced charge transfer	This work

Reference

1. J. H. Chong, M. Sauer, B. O. Patrick and M. J. MacLachlan, *Org. Lett.,* 2003, **5**, 3823-3826.
2. J. Liu, F. Yang, L. Cao, B. Li, K. Yuan, S. Lei and W. Hu, *Adv. Mater*., 2019, **31**, e1902264.
3. B. Sun, X. Li, T. Feng, S. Cai, T. Chen, C. Zhu, J. Zhang, D. Wang and Y. Liu, ACS Appl. Mater. Interfaces, 2020, **12**, 51837-51845.
4. C. Li, D. Li, W. Zhang, H. Li and G. Yu, Angew. Chem., Int. Ed., 2021, **60**, 27135-27143.
5. T. Li, H. Yu, Z. Xiong, Z. Gao, Y. Zhou and S.-T. Han, *Mater. Horiz.,* 2021, **8**, 2041-2049.
6. Y. Song, G. Feng, L. Wu, E. Zhang, C. Sun, D. Fa, Q. Liang, S. Lei, X. Yu and W. Hu, *J. Mater. Chem. C,* 2022, **10**, 2631-2638.
7. L. Liu, B. Geng, W. Ji, L. Wu, S. Lei and W. Hu, *Adv. Mater*., 2023, **35**, 2208377.
8. D. Wu, Q. Che, H. He, M. E. El-Khouly, S. Huang, X. Zhuang, B. Zhang and Y. Chen, *ACS Materials Lett.*, 2023, **5**, 874-883.